

Reinforcement Learning for Improved Random Access in Delay-Constrained Heterogeneous Wireless Networks

Lei Deng, *Member, IEEE*, Danzhou Wu, Zilong Liu, *Senior Member, IEEE*,
Yijin Zhang, *Senior Member, IEEE*, and Yunghsiang S. Han, *Fellow, IEEE*

Abstract

In this paper, we for the first time investigate the random access problem for a delay-constrained heterogeneous wireless network. We begin with a simple two-device problem where two devices deliver delay-constrained traffic to an access point (AP) via a common unreliable collision channel. By assuming that one device (called Device 1) adopts ALOHA, we aim to optimize the random access scheme of the other device (called Device 2). The most intriguing part of this problem is that Device 2 does not know the information of Device 1 but needs to maximize the system timely throughput. We first propose a Markov Decision Process (MDP) formulation to derive a model-based upper bound so as to quantify the performance gap of certain random access schemes. We then utilize reinforcement learning (RL) to design an R-learning-based random access scheme, called tiny state-space R-learning random access (TSRA), which is subsequently extended for the tackling of the general multi-device problem. We carry out extensive simulations to show that the proposed TSRA simultaneously achieves higher timely throughput, lower computation complexity, and lower power consumption than the existing baseline—deep-reinforcement learning multiple access (DLMA). This indicates that our proposed TSRA scheme

A preliminary version of this work was presented by IEEE GLOBECOM Workshop on Towards Native-AI Wireless Networks, 2021 [1]. (*Corresponding author: Yunghsiang S. Han.*)

L. Deng and D. Wu are with College of Electronics and Information Engineering, Shenzhen University, Shenzhen 518060, China (e-mail: ldeng@szu.edu.cn, wudanzhou2019@email.szu.edu.cn).

Z. Liu is with School of Computer Science and Electronic Engineering, University of Essex, Colchester CO4 3SQ, U.K. (e-mail: zilong.liu@essex.ac.uk).

Y. Zhang is with School of Electronic and Optical Engineering, Nanjing University of Science and Technology, Nanjing 210094, China (e-mail: yijin.zhang@gmail.com).

Y. S. Han is with Shenzhen Institute for Advanced Study, University of Electronic Science and Technology of China, Shenzhen 518110, China (e-mail: yunghsiangh@gmail.com).

is a promising means for efficient random access over massive mobile devices with limited computation and battery capabilities.

Index Terms

Delay-constrained wireless communication, heterogeneous network, random access, reinforcement learning.

I. INTRODUCTION

Wireless communications are rapidly evolving from connecting people to networking everything in various vertical industries. Toward that end, hard delay constraint is one of the most important communication requirements in many vertical applications, such as factory automation, robot collaboration, smart grid load control, autonomous vehicles, online gaming, virtual reality, and tactile Internet, etc. [2]–[9]. In such applications, each packet is assigned a hard delay: it will expire and then be removed from the system if it has not been delivered successfully within a given delay. For example, in virtual reality, the motion-to-photon latency is generally at most 15ms; exceeding this deadline will cause motion sickness and dizziness to the device [10]. This hard delay constraint poses an array of challenges to network design, since many existing techniques designed for legacy communication networks may not work well for delay-constrained ones [6].

To support various applications in different scenarios, heterogeneous wireless networks are ubiquitous nowadays where the heterogeneity comes from three aspects. First, massive number of devices serving a range of applications may have different traffic patterns. Second, there are a variety of channel conditions to be dealt with in wireless networks, in which the communication quality highly depends on radio propagation conditions such as distance, mobility, shadowing, and fading, etc. Third and most importantly, different communication protocols may need to be simultaneously supported in wireless networks. It is common that different networks, such as cellular (NB-IoT), LoRa, WiFi, Bluetooth, Zigbee, NFC, co-exist in certain area to deliver data traffic. To avoid/mitigate interference, most of the current spectrum bands are exclusively assigned among different networks. Such an exclusively-assigning scheme, however, is hard to satisfy the explosively increasing wireless traffic, since it is unable to dynamically match the supply and demand. To address this issue, the Defense Advanced Research Projects Agency (DARPA) envisions that spectrum should be dynamically and collaboratively shared by hetero-

geneous wireless networks. To validate this new spectrum sharing scheme, DARPA hosted a three-year competition, called Spectrum Collaboration Challenge (SC2), where teams need to design clean-slate radio techniques to share spectrum with their competitors but without knowing protocol details of competitors, *with the ultimate goal of increasing overall data throughput* [11], [12]. The competition has demonstrated that indeed the new collaboratively-sharing scheme can transmit far more data. To realize DARPA's vision, we need to re-design PHY, MAC and network layers of wireless networks. In this paper, we only focus on the MAC layer design, in particular, on the uplink random access scheme design, for heterogeneous wireless networks.

Several random access schemes have been designed in heterogeneous wireless networks under the delay-unconstrained settings. Yu *et al.* in [13] introduced deep reinforcement learning (DRL) into the random access scheme design for heterogeneous wireless networking. Their proposed scheme, called deep-reinforcement learning multiple access (DLMA), adopted feedforward neural networks (FNN) as the deep neural network. In [14], the authors further applied DRL into CSMA and designed a new CSMA variant, called CS-DLMA, for heterogeneous wireless networking. As compared with DLMA, CS-DLMA adopts recurrent neural networks (RNN) for a non-uniform time-step deep Q-network (DQN) by leveraging the fact that the time duration required for carrier sensing is smaller than the duration of data transmission. Both [13] and [14] assume a saturated delay-unconstrained traffic pattern. On the other hand, some works studied random access schemes for delay-constrained communication in homogeneous wireless networking. Deng *et al.* in [15] analyzed the asymptotic performance of ALOHA system for frame-synchronized delay-constrained traffic pattern. Zhang *et al.* in [16] studied the system throughput and optimal retransmission probability of ALOHA for the saturated delay-constrained traffic. Campolo *et al.* in [17] analyzed p -persistent CSMA for broadcasting delay-constrained traffic. An online-learning-based multiple access scheme, called Learn2MAC, was proposed in [18] to provide delay guarantee and low energy consumption. However, to the best of our knowledge, there have been no works designing uplink random access scheme for delay-constrained heterogeneous wireless networks.

In this paper, we take a first step to fill this blank by designing a reinforcement-learning-based random access scheme, called Tiny State-space **R**-learning random Access (TSRA), which delivers delay-constrained traffic in a heterogeneous wireless network. We show that TSRA simultaneously achieves higher timely throughput, lower computation complexity, and lower power consumption than existing baseline schemes, including DLMA [13] and Learn2MAC

TABLE I
A COMPARISON OF OUR PROPOSED TSRA SCHEME WITH EXISTING BASELINES.

Random Access Scheme	DLMA [13]	Learn2MAC [18]	ALOHA [15]	TSRA (This work)
Timely Throughput	Medium	Low	Low	High
Computation Complexity	High	Medium	Low	Low
Power Consumption	High	High	Low	Low
Methodology	Deep Reinforcement Learning	Online Learning	Simple Stochastic Model	R-Learning

[18], for a large number of settings with up to 100 devices. A comparison of our proposed TSRA with three existing baseline schemes is shown in Table I. As we can see, the proposed TSRA represents a promising enabling approach for efficient wireless networking where the devices may suffer from limited computation and battery capabilities.

The key idea of TSRA originates from a comprehensive analysis for a simple two-device problem where there are only two devices accessing a wireless channel for delivering delay-constrained traffic. Whilst one device (called Device 1) adopts the slotted ALOHA scheme, we optimize the random access scheme of the other (called Device 2) with the goal of maximizing the system timely throughput. Assuming that Device 2 does not know the information of Device 1, the primary objective here is how to maximize the system timely throughput. The analysis and proposed random access scheme for the simple two-device case can be naturally extended to the general multi-device case. Thus, in the rest of this paper, we will concentrate on such a two-device problem before describing the general multi-device problem. Specifically, our major contributions of this paper are summarized as follows:

- For the two-device case, we first establish a model-based upper bound, and then propose an average-reward model-free R-learning-based random access scheme [19]–[21]. We illustrate that the average-reward-based R-learning is more effective than the widely-used discounted-reward-based Q-learning for our problem. Since the state space of R-learning exponentially increases with D , we further exploit the problem structure and design the low-complexity TSRA scheme by only utilizing the information about whether Device 2 has a most urgent packet (which will expire in one slot).
- We further extend TSRA to the general multi-device case by carefully re-designing the reward function. Since there are significantly more system possibilities in the multi-device case, we show that the reward function with only two values in the two-device case is not

suitable for the general multi-device case. Instead, we design a more sophisticated reward function with four value levels to better differentiate different system possibilities.

- Finally, we conduct extensive simulations to demonstrate the superior performance of TSRA. For the two-device case, we show that the system timely throughput of TSRA is 5.62% higher than that of the existing baseline DLMA [13] and is only 4.98% lower than the derived upper bound. The time and space complexity of TSRA are respectively 96.36% and 83.62% lower than that of DLMA. For the multi-device case, TSRA increases the system timely throughput by 79.19% than DLMA, and the time and space complexity of TSRA are respectively 98.29% and 90.74% lower than that of DLMA. Furthermore, TSRA reduces the system power consumption by 52.29% as compared to DLMA.

The rest of this paper is organized as follows. In Secs. II-IV, we study the two-device problem in great detail and illustrate how we design the TSRA scheme. In particular, for the two-device problem, we describe the system model in Sec. II, derive an MDP-based upper bound for the performance in Sec. III, and propose the TSRA scheme in Sec. IV. In Sec. V, we extend TSRA to the general multi-device problem. In Sec. VI, we carry out extensive simulations to compare TSRA with existing baselines. Sec. VII concludes this paper.

II. SYSTEM MODEL AND PROBLEM FORMULATION: A TWO-DEVICE CASE

As we mentioned in the previous section, our proposed TSRA scheme is fundamentally derived from a simple two-device case. We thus first describe the system model and problem formulation for the two-device case in this section. The system model is depicted in Fig. 1. Specifically, two devices share a wireless channel to deliver delay-constrained traffic to an access point (AP). Time is slotted and indexed from slot 1. A slot spans the time duration for an device to transmit a packet to the AP and get a feedback from the AP. For easier reference, we use “at slot t ” to refer to “at the beginning of slot t ” and use “in slot t ” to refer to “in the time space of slot t ”. System state changes at a slot and transmission behaviour occurs in a slot. To facilitate the analysis, we first assume a delay-constrained Bernoulli traffic pattern for both devices: Device 1 (resp. Device 2) has a new packet arrival with probability $p_b \in (0, 1]$ (resp. $p'_b \in (0, 1]$) at any slot, and all packets have a hard delay of D slots. Note that the Bernoulli arrivals characterized by an arrival rate p_b or p'_b are widely used in wireless communication research, e.g., [22]–[24]. A packet will be removed from the system if it has not been delivered successfully to the AP in D slots after its arrival. We will later investigate different traffic patterns in Sec. VI.

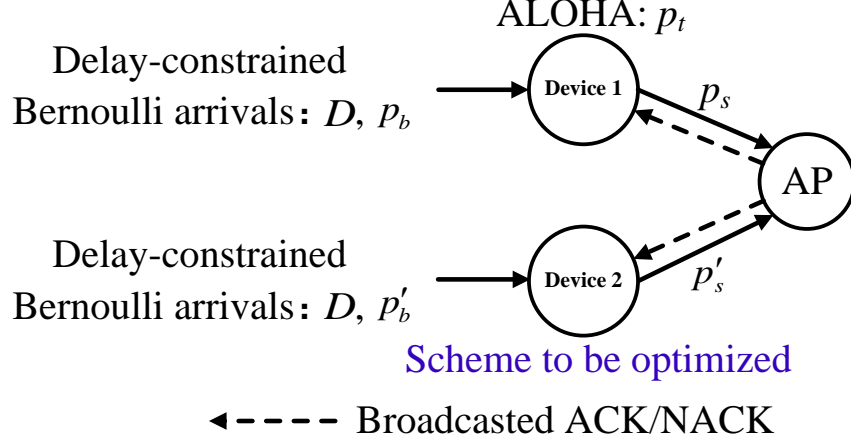


Fig. 1. System model for the two-device case.

We assume an *unreliable collision* wireless channel model. If both devices transmit a packet to the AP in a slot, then a channel collision occurs and both packets cannot be successfully received/decoded by the AP. Even though only one device transmits a packet to the AP, the wireless channel is still unreliable due to shadowing and fading. We model such unreliability by a success probability. Specifically, if only Device 1 (resp. Device 2) transmits a packet to the AP, the packet can be successfully delivered with probability $p_s \in (0, 1]$ (resp. $p'_s \in (0, 1]$). Otherwise, a channel error happens. Thus, a transmission failure may occur either due to a channel collision or due to a channel error. Note that we model an unreliable channel by a parameter p_s or p'_s , which is also widely used in delay-constrained wireless communications, e.g., [6], [25]–[27].

The two-device network is heterogeneous, not only because they could have different arrival probabilities and different channel success probabilities, but also because they may use different random access schemes (i.e., transmission policies). We assume that Device 1 adopts the slotted ALOHA¹ protocol with transmission/retransmission probability $p_t \in [0, 1]$. Namely, Device 1 always transmits or retransmits its head-of-line (HoL) packet to the AP with probability p_t in any slot. The random access scheme of Device 2 is under our control. We design its random access scheme π so as to maximize the system timely throughput [15], which is defined as

$$R^\pi \triangleq \liminf_{T \rightarrow \infty} \frac{\mathbb{E}^\pi [\text{\# of packets of both devices delivered successfully before expiration from slot 1 to slot } T]}{T}. \quad (1)$$

¹For simplicity, we will use “ALOHA” to represent “slotted ALOHA” in the rest of this paper.

The expectation is taken over all system randomness and possibly policy randomness. Note that our design space is Device 2's scheme while our goal is to maximize the system timely throughput. This is in line with DARPA's vision on collaboratively-sharing scheme for spectrum [11], [12].

Note that both devices cannot communicate with each other. Thus, Device 2 does not know the queue information and transmission information of Device 1. However, it can interact with the environment (i.e., the AP) to learn the information of Device 1. Specifically, at the end of a slot, the AP will broadcast an acknowledgement (ACK) to both devices if it successfully decodes a packet, broadcast a negative-acknowledgement (NACK) if it receives at least one packet but does not decode it successfully (either due to a channel collision or due to a channel error), and broadcast nothing if it does not receive any packet in this slot. By observing such feedback, Device 2 aims to infer the behaviour of Device 1 and then judiciously design its access scheme. This motivates us to use reinforcement learning (RL) [21] due to its great success in solving many interactive decision problems in a model-free manner.

III. A MODEL-BASED UPPER BOUND FOR THE TWO-DEVICE CASE

Before we present our model-free RL-based random access scheme in Sec. IV, we present a model-based upper bound for the two-device case in this section. Suppose that Device 2 is aware of Device 1's parameters including p_b , D , p_t , and p_s , and queue information (i.e., the number of packets in the queue and the arrival time of each packet) at the beginning of any slot. However, when Device 2 decides to transmit or not transmit a packet in any slot, it cannot know whether Device 1 transmits/retransmits a packet or not in the same slot. Otherwise, Device 2 can always avoid collision such that the problem becomes trivial. Such a model-based setting with more revealed information to Device 2 allows us to derive an upper bound for the system timely throughput of the original model-free problem. This upper bound will serve as a performance benchmark for evaluating any random access policy later, as we can numerically gauge the performance gap.

We first consider the special case of the hard delay $D = 1$. Note that $D = 1$ means that any packet arriving at (the beginning of) slot t will expire at the end of slot t (i.e., at the beginning of slot $t + 1$) if it is not transmitted or its transmission fails due to channel collision or channel error. Thus, at any slot, the queue of both devices has at most one packet. This significantly simplifies the system design due to the coupling-free feature between different slots. We can

thus derive the optimal policy of Device 2, which surprisingly is a binary policy, as shown in the following theorem.

Theorem 1: If $D = 1$, then the optimal strategy of Device 2 to maximize the system timely throughput is i) always transmitting the HoL packet if

$$p_b p_t < \frac{p'_s}{p_s + p'_s}, \quad (2)$$

and ii) always remaining idle if its queue is empty or (2) does not hold. The corresponding system timely throughput is

$$R = \begin{cases} [p'_s - (p_s + p'_s)p_t p_b] p'_b + p_s p_t p_b, & \text{if (2) holds;} \\ p_s p_t p_b, & \text{otherwise.} \end{cases} \quad (3)$$

Proof: Please see the proof in Appendix A. ■

Let us investigate condition (2) by assuming that $p_s = p'_s$, i.e., both devices have the same channel quality. In this case, condition (2) becomes $p_b p_t < 0.5$. Note that $p_b p_t$ is the probability that Device 1 transmits a packet in any slot since $D = 1$. Thus, if this probability is less than 0.5, i.e., Device 1 is not aggressive, Device 2 will become completely aggressive to take over the channel. Conversely, if this probability is larger than 0.5, i.e., Device 1 is aggressive, Device 2 will become completely unaggressive to hand over the channel. Such a binary policy achieves the best tradeoff between utilizing the wireless channel and avoiding collision. The closed-form expression (3) serves as an upper bound for $D = 1$.

However, for general $D > 1$, it is difficult to directly characterize an optimal strategy and the corresponding system timely throughput because of the coupling feature between different slots. Since both the Bernoulli traffic pattern and the collision channel are memoryless and the queue dynamics only depend on its current state, our system preserve the Markov property. We thus formulate our problem as an MDP problem and propose an upper bound by numerically solving a linear programming problem. An MDP is characterized by its state, action, reward function, and transition probability [28]. The state of the system at (the beginning of) slot t is defined as

$$s_t \triangleq (l_{t,1}, l_{t,2}, o_t). \quad (4)$$

In (4), $l_{t,i} = (l_{t,i}^1, l_{t,i}^2, \dots, l_{t,i}^D)$ is the lead time vector [6] of Device $i \in \{1, 2\}$ at slot t , where

$$l_{t,i}^k = \begin{cases} 1, & \text{if Device } i \text{ has a packet at slot } t, \text{ which will expire in } k \in \{1, 2, \dots, D\} \text{ slots;} \\ 0, & \text{otherwise.} \end{cases}$$

TABLE II

THE INTERPRETATION OF FOUR DIFFERENT CHANNEL OBSERVATIONS, DEPENDING ON WHETHER DEVICE 2 TRANSMITS A PACKET OR NOT.

Observation o_t	Device 2 transmits a packet in slot $t - 1$	Device 2 does not transmit a packet in slot $t - 1$
IDLE	Impossible	Device 1 does not transmit a packet in slot $t - 1$
BUSY	Impossible	Device 1 transmits a packet in slot $t - 1$, and no channel error happens for Device 1
SUCCESSFUL	Device 1 does not transmit a packet in slot $t - 1$, and no channel error happens for Device 2	Impossible
FAILED	Device 1 transmits a packet in slot $t - 1$ and a channel collision happens, or Device 1 does not transmit a packet and a channel error happens for Device 2	Device 1 transmits a packet in slot $t - 1$, and a channel error happens for Device 1

Further, $o_t \in \{\text{BUSY}, \text{SUCCESSFUL}, \text{IDLE}, \text{FAILED}\}$ is the channel observation at (the beginning of) slot t , equivalently, at the end of slot $t - 1$. Depending on whether devices transmit a packet in slot $t - 1$, the interpretation of these four different observations is shown in Table II. Specifically, channel observation $o_t = \text{IDLE}$ means that Device 2 receives nothing from the AP at the end of slot $t - 1$, indicating that both devices do not transmit a packet in slot $t - 1$. Channel observation $o_t = \text{BUSY}$ means that Device 2 does not transmit a packet but receives an ACK from the AP in slot $t - 1$, indicating that Device 1 transmits a packet and no channel error happens for Device 1's packet. Channel observation $o_t = \text{SUCCESSFUL}$ means that Device 2 transmits a packet and receives an ACK from the AP in slot $t - 1$, indicating that Device 1 does not transmit a packet and no channel error happens for Device 2's packet. Channel observation $o_t = \text{FAILED}$ means that Device 2 receives a NACK from the AP in slot $t - 1$. This is the most complicated observation and it has two different interpretations. If Device 2 does not transmit a packet in slot $t - 1$, this observation means that Device 1 transmits a packet and a channel error happens in slot $t - 1$. If Device 2 transmits a packet in slot $t - 1$, this observation means that a channel collision or a channel error happens in slot $t - 1$ (Device 2 cannot distinguish these two possibilities). Without loss of generality, we assume that $o_1 = \text{IDLE}$. We remark that the modeling for channel observation is the same as [13]. The set of all possible states is denoted by \mathcal{S} . Clearly, we have $|\mathcal{S}| = 2^D \cdot 2^D \cdot 4 = 2^{2D+2}$.

In slot t , the action of Device 2 is denoted by a_t . Similar to [13], the action space is defined as $\mathcal{A} \triangleq \{\text{TRANSMIT}, \text{WAIT}\}$. One can readily prove that it is optimal to first transmit the HoL packet if there are multiple packets in the Device 2's queue at any slot. Thus, action

$a_t = \text{TRANSMIT}$ means that Device 2 transmits its HoL packet in slot t , while $a_t = \text{WAIT}$ means that Device 2 does not transmit a packet in slot t .

We define the reward function $r(s_t, a_t)$ as

$$r(s_t, a_t) \triangleq 1_{\{o_t \in \{\text{BUSY}, \text{SUCCESSFUL}\}\}}, \forall s_t \in \mathcal{S}, a_t \in \mathcal{A}, \quad (5)$$

where $1_{\{\cdot\}}$ is the indicator function. Note that $o_t = \text{BUSY}$ means that Device 1 transmits a packet successfully in slot $t - 1$, and $o_t = \text{SUCCESSFUL}$ means that Device 2 transmits a packet successfully in slot $t - 1$. Thus $r(s_t, a_t) = 1$ if the system (either Device 1 or Device 2) transmits a packet successfully in slot $t - 1$. Note that we model the reward with “delay of gratification”. Namely, the delivered packet in slot $t - 1$ is translated into the reward at slot t . However, since our performance metric is long-term system timely throughput, such “delay of gratification” will not cause performance loss, as shown in (7) later. In addition, we remark that the reward function only depends on the channel observation o_t , regardless of queue information $l_{t,1}$ and $l_{t,2}$.

The transition probability from state s at slot t to state s' at slot $t + 1$ if taking action a in slot t is defined as

$$P(s'|s, a) \triangleq P(s_{t+1} = s' | s_t = s, a_t = a), \forall t, s, s', a, \quad (6)$$

which depends on (i) the arrival and expiration events of both devices, (ii) the transmission events of both devices, (iii) the channel collision and channel error events, and (iv) the change of lead time vector. We use an example to illustrate how to compute the transition probabilities; see https://github.com/DanzhouWu/TSRA/tree/main/two_device/TransitionProbability.

Based on the above MDP model, it is straightforward to see that the system timely throughput under a policy π defined in (1) is equivalent to the average reward of our formulated MDP under policy π , i.e.,

$$\begin{aligned} R^\pi &= \liminf_{T \rightarrow \infty} \frac{\mathbb{E}^\pi [\text{\# of packets of both devices delivered successfully before expiration from slot 1 to slot } T]}{T}, \\ &= \liminf_{T \rightarrow \infty} \frac{\sum_{t=2}^{T+1} \mathbb{E}^\pi \{r(s_t, a_t)\}}{T}, \\ &= \liminf_{T \rightarrow \infty} \frac{\sum_{t=1}^T \mathbb{E}^\pi \{r(s_t, a_t)\}}{T}. \end{aligned} \quad (7)$$

Again, note that the expectation is taken over all system randomness and possibly policy randomness. Thus, our problem becomes an average-reward MDP problem. Here we use the dual linear program approach to solve this MDP problem [28, Chapter 9.3],

$$\begin{aligned}
& \max \quad \sum_{s \in \mathcal{S}} \sum_{a \in \mathcal{A}} r(s, a) x(s, a) \\
& \text{s.t.} \quad \sum_{a \in \mathcal{A}} x(s', a) = \sum_{s \in \mathcal{S}} \sum_{a \in \mathcal{A}} P(s'|s, a) x(s, a), \quad \forall s' \in \mathcal{S} \\
& \quad \sum_{a \in \mathcal{A}} x(s', a) + \sum_{a \in \mathcal{A}} y(s', a) = \sum_{s \in \mathcal{S}} \sum_{a \in \mathcal{A}} P(s'|s, a) y(s, a) + \alpha_{s'}, \quad \forall s' \in \mathcal{S} \\
& \text{var.} \quad x(s, a) \geq 0, \quad y(s, a) \geq 0, \quad \forall s \in \mathcal{S}, a \in \mathcal{A}
\end{aligned} \tag{8}$$

where $\{\alpha_s : s \in \mathcal{S}\}$ are arbitrary constants such that $\alpha_s > 0$ ($\forall s \in \mathcal{S}$) and $\sum_{s \in \mathcal{S}} \alpha_s = 1$. Note that we follow standard procedures of the dual linear program in [28, Chapter 9.3]. Basically, notation $x(s, a)$ (resp. $y(s, a)$) represents the frequency (or the stationary probability) that the Markov chain is on state s and the action is a where s is a recurrent state (resp. a transient state); see [28, Proposition 9.3.2].

The optimal value of problem (8) serves as an upper bound for the system timely throughput for general $D > 1$. In addition, according to [29] and [28, Chapter 9.3.1], solving problem (8) also yields a randomized optimal policy,

$$\pi(a|s) = \begin{cases} \frac{x^*(s, a)}{\sum_{a \in \mathcal{A}} x^*(s, a)}, & \text{if } \sum_{a \in \mathcal{A}} x^*(s, a) > 0; \\ \frac{y^*(s, a)}{\sum_{a \in \mathcal{A}} y^*(s, a)}, & \text{otherwise.} \end{cases} \tag{9}$$

where $\pi(a|s)$ is the probability of taking action $a \in \mathcal{A}$ under state $s \in \mathcal{S}$, and $\{(x^*(s, a), y^*(s, a)) : s \in \mathcal{S}, a \in \mathcal{A}\}$ is an optimal solution of problem (8).

IV. TINY STATE-SPACE R-LEARNING RANDOM ACCESS (TSRA) SCHEME FOR THE TWO-DEVICE CASE

The disadvantage of model-based MDP is that Device 2 needs to know Device 1's parameters and queue information. However, such information cannot be obtained in practice such that Device 2 cannot know Device 1's queue state $l_{t,1}$ and the transition probabilities $P(s'|s, a)$ (Please refer to (4) and (6)). To address this issue, reinforcement learning (RL) has been proposed as a model-free approach to solve MDP problems. RL needs the state space \mathcal{S} , the action space \mathcal{A} , and the reward function $r(s, a)$, $\forall s \in \mathcal{S}, a \in \mathcal{A}$, but does not need the transition probabilities $P(s'|s, a)$ of an MDP. Instead, RL learns the model by directly interacting with the environment.

Since Device 2 cannot know Device 1's queue information, we define its state at slot t as²,

$$s_t \triangleq (l_{t,2}, o_t), \quad (10)$$

where $l_{t,2}$ is the queue information of Device 2 itself, and o_t is the channel observation (same as Sec. III). The state space \mathcal{S}' is thus of size $2^D \cdot 4 = 2^{D+2}$. The action space $\mathcal{A} = \{\text{TRANSMIT}, \text{WAIT}\}$ is again the same as that in Sec. III. The reward function $r(s_t, a_t)$ is defined as

$$r(s_t, a_t) \triangleq 1_{\{o_t \in \{\text{BUSY}, \text{SUCCESSFUL}\}\}}, \forall s_t \in \mathcal{S}', a_t \in \mathcal{A}, \quad (11)$$

which is similar to that in the model-based setting (Please refer to (5)). Namely, the reward is 1 if Device 2 receives an ACK, either for its own packet ($o_t = \text{SUCCESSFUL}$) or for Device 1's packet ($o_t = \text{BUSY}$). Otherwise, the reward is 0.

A. Q-Learning

Based on the above information, we can apply different RL methods to solve our problem in a model-free manner, such as Monte Carlo and temporal-difference learning [21]. Among them, Q-learning is one of the most widely-used methods [21]. In fact, the delay-unconstrained counterpart of our problem, i.e., [13], also used Q-learning. The simplest form of Q-learning, called one-step Q-learning, iteratively updates the Q-function $Q(s, a)$ as follows,

$$Q(s_t, a_t) \leftarrow Q(s_t, a_t) + \alpha [r(s_t, a_t) + \gamma \max_{a \in \mathcal{A}} Q(s_{t+1}, a) - Q(s_t, a_t)], \quad (12)$$

where $\alpha \in (0, 1]$ is the learning rate, $\gamma \in (0, 1)$ is the discount factor, and $Q(s, a)$ is the state-action value function (called Q-function), approximating the discounted reward for given state and action for the iteratively updated policy π , i.e.,

$$Q(s, a) \approx \mathbb{E}^\pi \left[\sum_{\tau=t}^{\infty} \gamma^{\tau-t} r(s_\tau, a_\tau) | s_t = s, a_t = a \right]. \quad (13)$$

Note that the policy π is iteratively updated by selecting action a to maximize $Q(s, a)$ for any state s with an ϵ -greedy algorithm [21]. We call the algorithm **Full State-space Q-learning random Access (FSQA)**, which is detailed in Algorithm 1.

Q-learning is suitable for solving MDPs with discounted reward in a model-free manner. However, in network communication research, the major performance metric, throughput or

²With a little bit abuse of notation, in the model-free problem in this section, except for the state space, we adopt the same notations of the model-based problem in Sec. III. Namely, we still use s_t to denote the state, a_t to denote the action, and $r(s_t, a_t)$ to denote the reward function for the model-free problem in this section. They are distinguishable in the context.

Algorithm 1 FSQA Algorithm for Device 2 in the Two-Device Problem

1: Initialize Q-function $Q(s, a) = 0, \forall s \in \mathcal{S}', \forall a \in \mathcal{A}$,

2: Set learning rate $\alpha = 0.01$

3: Initialize the discount factor $\gamma = 0.9$

4: Observe the initial system state s_1

5: **for** $t = 1, 2, \dots$ **do**

6: Choose a_t with an ϵ -greedy algorithm, i.e.,

$$a_t = \begin{cases} \arg \max_{a \in \mathcal{A}} Q(s_t, a), & \text{with prob. } 1 - \epsilon_t; \\ \text{random action,} & \text{with prob. } \epsilon_t, \end{cases}$$

where $\epsilon_t = \max\{0.995^{t-1}, 0.01\}$

7: Observe $r(s_t, a_t), s_{t+1}$

8: Update Q-function as follows,

$$Q(s_t, a_t) \leftarrow Q(s_t, a_t) + \alpha(r(s_t, a_t) + \gamma \max_{a \in \mathcal{A}} Q(s_{t+1}, a) - Q(s_t, a_t))$$

9: **end for**

timely throughput, is a long-term average reward. Therefore, Q-learning may be less suitable for network communication research than another RL method, called R-learning, which solves MDPs with average reward in a model-free manner [19]–[21].

B. R-Learning

R-learning also utilizes the state-action value function (we still call it Q-function by convention), which however has a different meaning. Among the variants of R-learning [19]–[21], in this paper, we adopt the version in [20, Algorithm 3] and [21, Figure 11.2],

$$Q(s_t, a_t) \leftarrow Q(s_t, a_t) + \alpha[r(s_t, a_t) + \max_{a \in \mathcal{A}} Q(s_{t+1}, a) - Q(s_t, a_t) - \rho], \quad (14)$$

$$\rho \leftarrow \rho + \beta[r(s_t, a_t) + \max_{a \in \mathcal{A}} Q(s_{t+1}, a) - Q(s_t, a_t) - \rho], \quad (15)$$

where $\alpha \in (0, 1]$ and $\beta \in (0, 1]$ are learning rates, ρ approximates the state-independent average reward for the iteratively updated policy π , i.e.,

$$\rho \approx \lim_{T \rightarrow \infty} \mathbb{E}^\pi \left[\frac{\sum_{t=1}^T r(s_t, a_t)}{T} \right], \quad (16)$$

and Q-function $Q(s, a)$ approximates the state-dependent cumulative reward difference (called relative value in [20], [21]) for the iteratively updated policy π , i.e.,

$$Q(s, a) \approx \mathbb{E}^{\pi} \left[\sum_{\tau=t}^{\infty} [r(s_{\tau}, a_{\tau}) - \rho] \middle| s_t = s, a_t = a \right]. \quad (17)$$

Similar to Q-learning, the policy π is iteratively updated by selecting action a to maximize $Q(s, a)$ for any state s with an ϵ -greedy algorithm. We call the algorithm **Full State-space R-learning random Access (FSRA)**, which is detailed in Algorithm 2.

We compare FSQA and FSRA by varying D from 1 to 10. For each D , we randomly select 500 groups of different system parameters, i.e., $(p_b, p'_b, p_s, p'_s, p_t)$. For each group of parameters, we simulate 10,000,000 slots independently for FSQA and FSRA, and evaluate the system timely throughput for the last 100,000 slots. The result is shown in Fig. 2. As we can see, FSRA outperforms FSQA for all D 's, suggesting that indeed R-learning is more suitable to our problem than Q-learning. As we explained before, R-learning is used to solve model-free MDPs with average reward, while Q-learning is used to solve model-free MDPs with discounted reward. Our problem turns out to be exactly a model-free MDP with average reward. That is the main reason that FSRA outperforms FSQA. In Appendix B, we further present an example to compare the policies of FSRA and FSQA after convergence and explicitly show that FSRA is better than FSQA. We also propose a method to tune FSQA so as to improve its performance.

In addition, we remark that FSQA is more difficult to converge than FSRA. As the hard delay D increases, we should expect that the system timely throughput also increases since packets have longer lifetime and thus are more difficult to expire. However, as D increases, the state space \mathcal{S}' (of size 2^{D+2}) also increases exponentially. As a result, both FSRA and FSQA need more slots to converge. But FSQA is much more sensitive to the state-space explosion. When $D \geq 4$, FSQA cannot converge in 10,000,000 slots such that its system timely throughput even decreases as D increases, as shown in Fig. 2. We will explicitly compare the convergence speeds of FSQA and FSRA in Sec. IV-C.

Although FSRA outperforms FSQA in terms of both the achieved system timely throughput and the convergence speed, we point out that FSRA still converges slowly as D increases. For example, in Fig. 2, we need to run 10,000,000 slots such that FSRA converges. This problem is even more severe when D is larger since the state space \mathcal{S}' (of size 2^{D+2}) increases exponentially with the hard delay D . Please refer to Sec. IV-C to see the slow convergence speed of FSRA. This disadvantage is not acceptable for dynamic heterogeneous wireless networks, since a small

Algorithm 2 FSRA/HSRA/TSRA Algorithm for Device 2 in the Two-Device Problem

- 1: Initialize Q-function $Q(s, a) = 0, \forall a \in \mathcal{A}, \forall s \in \tilde{\mathcal{S}}$, where the state space $\tilde{\mathcal{S}}$ is different for different algorithms,

$$\tilde{\mathcal{S}} = \begin{cases} \mathcal{S}', & \text{If the algorithm is FSRA;} \\ \mathcal{S}'', & \text{If the algorithm is HSRA;} \\ \mathcal{S}''', & \text{If the algorithm is TSRA;} \end{cases}$$

- 2: Initialize $\rho = 0$
 3: Set learning rates $\alpha = 0.01, \beta = 0.01$
 4: Observe the initial system state s_1
 5: **for** $t = 1, 2, \dots$ **do**
 6: Choose a_t with an ϵ -greedy algorithm, i.e.,

$$a_t = \begin{cases} \arg \max_{a \in \mathcal{A}} Q(s_t, a), & \text{with prob. } 1 - \epsilon_t; \\ \text{random action,} & \text{with prob. } \epsilon_t, \end{cases}$$

where $\epsilon_t = \max\{0.995^{t-1}, 0.01\}$

- 7: Observe $r(s_t, a_t), s_{t+1}$
 8: Update Q-function as follows,

$$Q(s_t, a_t) \leftarrow Q(s_t, a_t) + \alpha \left[r(s_t, a_t) + \max_{a \in \mathcal{A}} Q(s_{t+1}, a) - Q(s_t, a_t) - \rho \right]$$

- 9: Update ρ as follows,

$$\rho \leftarrow \rho + \beta \left[r(s_t, a_t) + \max_{a \in \mathcal{A}} Q(s_{t+1}, a) - Q(s_t, a_t) - \rho \right]$$

- 10: **end for**
-

change of the network could cause the system to take a long time to re-converge. To address this problem, we further explore the problem structure and significantly reduce the state space. As we mentioned in Sec. III, it is optimal to first transmit the HoL packet (the most urgent packet) if there are multiple packets in the Device 2's queue at any slot. Thus, we can imagine that the HoL packet has the biggest impact on the system performance. In fact, [30] has applied this idea to derive a near-optimal heuristic scheduling policy only based on the lead time of the HoL

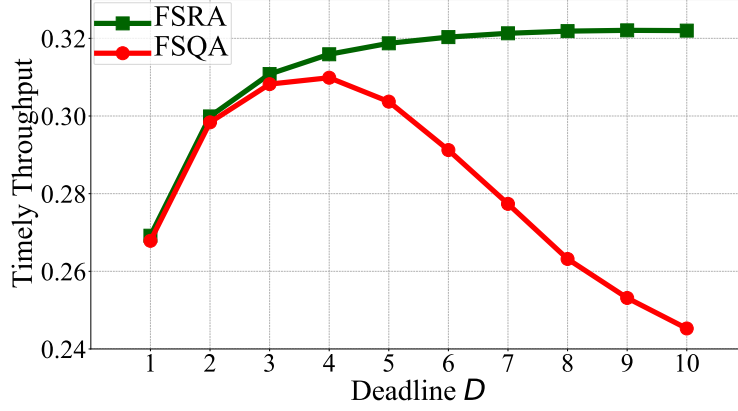


Fig. 2. Comparison of the system timely throughputs of FSRA and FSQA for the two-device problem.

packet for wireless downlink with deadline and retransmission constraints. We can also design a new R-learning random access algorithm only based on the lead time of the HoL packet. Namely, the state of Device 2 at slot t becomes

$$s_t \triangleq (h_{t,2}, o_t), \quad (18)$$

where $h_{t,2}$ is the lead time of the HoL packet of Device 2 at slot t and it is 0 by convention if Device 2 does not have any packet at slot t . The state space is denoted by \mathcal{S}'' , which is of size $4(D+1)$. The R-learning based algorithm is the same as FSRA except that the state space changes from \mathcal{S}' to \mathcal{S}'' . We call this algorithm **HoL**-packet-based **State-space R**-learning random Access (HSRA), which is detailed in Algorithm 2.

We can be even more aggressive by only considering if Device 2 has a packet whose lead time is 1. A packet with lead time 1 means that it will be expire at the end of the current slot if it cannot be delivered successfully in the current slot. Thus, such a packet is the most urgent one among all packets in the system. Therefore, we re-define the system state of Device 2 as

$$s_t \triangleq (f_{t,2}, o_t), \quad (19)$$

where

$$f_{t,2} = \begin{cases} 1, & \text{if Device 2 has a packet whose lead time is 1 at slot } t; \\ 0, & \text{otherwise.} \end{cases} \quad (20)$$

The state space is denoted by \mathcal{S}''' whose size is only 8 now. Since the state space is quite small and even not related to the hard delay D , we call this algorithm **Tiny State-space R**-learning

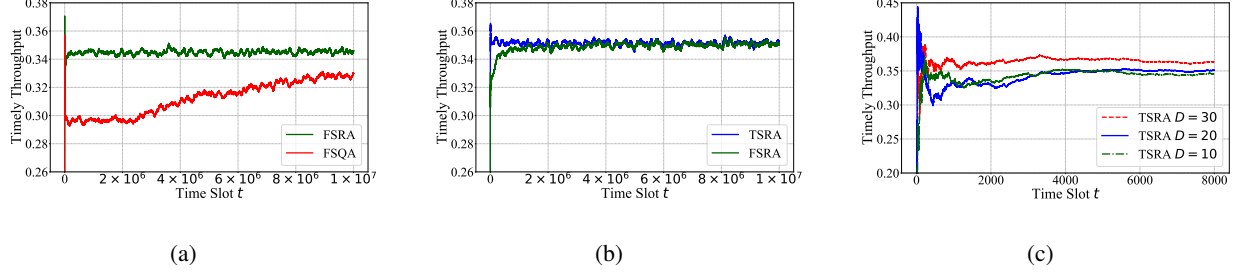


Fig. 3. Comparison of the convergence speeds of different schemes for the two-device problem. (a) FSRA v.s. FSQA with $D = 5$. (b) TSRA v.s. FSRA $D = 10$. (c) TSRA with three different hard delay values.

Random Access (TSRA). Again, TSRA is the same as FSRA except that the state space changes from \mathcal{S}' to \mathcal{S}''' , which is also detailed in Algorithm 2. Since the state space of TSRA is quite small, it converges much faster than FSRA, as shown in Sec. IV-C shortly. We will also show that its performance is close to HSRA and FSRA in Sec. VI. Thus, this is the final designed policy for our studied two-device problem in Sec. II. We will also extend TSRA to the general multi-device problem in Sec. V.

C. Comparing Convergence Speeds of FSQA, FSRA and TSRA

In this subsection, we compare the convergence speeds of FSQA, FSRA and TSRA. We set the system parameters to be $p_b = 0.5$, $p'_b = 0.4$, $p_s = 0.7$, $p'_s = 0.6$, $p_t = 0.4$,

We first show that FSQA is more difficult to converge than FSRA with $D = 5$. The result is shown in Fig. 3(a). We can observe that FSRA converges in 200,000 slots, while FSQA does not converge at the end of the simulation. Namely, FSQA cannot converge in 10,000,000 slots in this example, which indeed demonstrates that FSQA is very difficult to converge.

We next show that FSRA is more difficult to converge than TSRA with a larger hard delay $D = 10$. The result is shown in Fig. 3(b). We can observe that TSRA converges much faster than FSRA, and its achieved system timely throughput after convergence is almost the same as that of FSRA.

We can further enlarge the hard delay D and show that TSRA still converges very fast. We let D be 10, 20, and 30, respectively. The result is shown in Fig. 3(c). We can observe that TSRA converges in 6,000 slots for all three cases. The fast convergence speed of TSRA makes it suitable in practical dynamic heterogeneous networks.

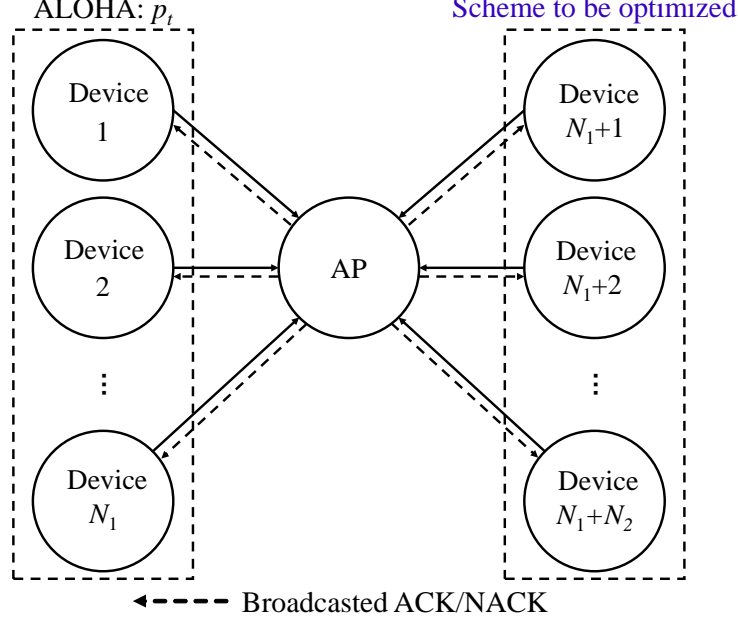


Fig. 4. The system model for the multi-device case.

V. EXTENSION TO THE MULTI-DEVICE CASE

In the previous three sections, we illustrated how and why we design TSRA for a delay-constrained heterogeneous wireless network with only two devices. However, the number of devices in a wireless network could be in the order of hundreds or even thousands. Thus, we should investigate how to design a random access scheme for the general multi-device problem. Fortunately, we will soon show that TSRA after slightly modifying the reward function still works well for the general multi-device problem.

Similar to the two-device problem, the system model for the multi-device problem is shown in Fig. 4. We assume that there are in total N devices (denoted by set \mathcal{N}). Among them, the first N_1 devices (denoted by set \mathcal{N}_1) are out of our control, and we assume that they use ALOHA protocol with the same transmission/retransmission probability p_t for simplicity. The rest of $N_2 = N - N_1$ devices (denoted by set $\mathcal{N}_2 \triangleq \mathcal{N} \setminus \mathcal{N}_1$) are under our control, and we should design a random access scheme for them. For example, they could use ALOHA, DLMA, or FSRA/HSRA/TSRA. In this work, we directly apply the TSRA scheme designed for the two-device problem (see Sec. IV) to this multi-device problem. Specifically, similar to (19), the state

TABLE III
THE NEW REWARD FUNCTION FOR ANY DEVICE $i \in \mathcal{N}_2$ FOR THE MULTI-DEVICE PROBLEM.

Observation o_t	$a_{t-1,i} = \text{TRANSMIT}$		$a_{t-1,i} = \text{WAIT}$	
	$f_{t-1,i} = 1$	$f_{t-1,i} = 0$	$f_{t-1,i} = 1$	$f_{t-1,i} = 0$
IDLE	Impossible	Impossible	-3	2
BUSY	Impossible	Impossible	10	10
SUCCESSFUL	10	10	Impossible	Impossible
FAILED	-5	-5	2	2

of any Device $i \in \mathcal{N}_2$ at slot t is defined as

$$s_t \triangleq (f_{t,i}, o_t), \quad (21)$$

where

$$f_{t,i} = \begin{cases} 1, & \text{if Device } i \text{ has a packet whose lead time is 1 at slot } t; \\ 0, & \text{otherwise.} \end{cases} \quad (22)$$

In addition, the action of any Device $i \in \mathcal{N}_2$ at slot t is defined as $a_{t,i} \in \{\text{TRANSMIT}, \text{WAIT}\}$.

The TSRA scheme is also the same as that in Algorithm 2.

However, we remark that we cannot simply apply the reward function in (11) to the multi-device case. In (11), we have only two reward values. The reward is 1 if the channel observation is BUSY or SUCCESSFUL, while the reward is 0 if the channel observation is IDLE or FAILED. This two-level reward function works well for the simple two-device problem. But later in Fig. 8(b), we will show that TSRA with this two-level reward function could have very bad performance. The main reason is the multi-device problem is much more complicated than the two-device problem. The multi-device system has many more system possibilities than the two-device problem. For example, if a device in \mathcal{N}_2 observes channel state FAILED and it does not transmit a packet, in the two-device case, the only reason is that the other device (i.e., Device 1) transmits a packet and a channel error happens. However, in the multi-device case, another reason is that more than two other devices simultaneously transmit a packet and thus a channel collision happens. We should use a more sophisticated reward function with more value levels to better differentiate such different system possibilities. We thus design a new reward function as shown in Table III. Later in Fig. 8(c), we will show that TSRA with this modified multi-level reward function works much better than the simple two-level reward function in (11).

In addition, we remark that we cannot control the devices in \mathcal{N}_1 who use ALOHA. At any slot t , if at least one device in \mathcal{N}_1 transmits a packet, all devices in \mathcal{N}_2 cannot have a successful

transmission in this slot. Instead, such devices in \mathcal{N}_2 can even jeopardize the transmission of devices in \mathcal{N}_1 if they join the competition. In other words, If the uncontrollable devices in \mathcal{N}_1 are already very congested such that there is no room for other devices to join the competition, then there is no significant benefit to add TSRA devices. Therefore, we should focus on the case that the uncontrollable devices in \mathcal{N}_1 are not so congested. In the extreme case, we should consider that $N_1 = 0$, i.e., no ALOHA devices but only TSRA devices exist in the system. This problem is very interesting and important, because it can examine if multiple TSRA devices can collaborate with each other. Later in Sec. VI, we will first evaluate the performance of the extreme case $N_1 = 0$ and then evaluate the performance of light-loaded cases with $N_1 = 1, 2, 3$.

VI. SIMULATIONS

In this section, we carry out extensive simulations to validate the effectiveness of our proposed random access scheme TSRA and demonstrate that TSRA outperforms the existing baselines, including DLMA, which is the random access scheme adopted by [13] for delay-unconstrained heterogeneous wireless networks, and Learn2MAC, which is an online-learning-based random access scheme proposed in [18] to provide delay guarantee and low energy consumption for homogeneous wireless networks with frame-synchronized delay-constrained traffic patterns and perfect channel. We implement all algorithms and evaluate their performances using Python language (7K+ lines of code). All evaluations are conducted in a computer with two CPUs (Intel Xeon E5-2678 v3), one GPU (NVIDIA GeForce GTX 2080 Ti), and 64GB memory, running Ubuntu 16.04.6 LTS. All source codes are publicly available in <https://github.com/DanzhouWu/TSRA>.

In the following, we will separately show the simulation results for the two-device case and the multi-device case.

A. Two-Device Case

We first demonstrate the performance of our proposed schemes for the two-device problem.

Timely Throughput Comparison. We first compare all our proposed random access algorithms, including the upper-bound algorithm, i.e., (9), FSRA/HSRA/TSRA proposed in Sec. IV, and the existing baselines, DLMA [13] and Learn2MAC [18]. We simulate the hard delay D from 1 to 30. For each D , we randomly select 500 groups of system parameters $(p_b, p'_b, p_s, p'_s, p_t)$, and independently run each group for 10,000,000 slots for FSRA and 100,000 slots for the other five algorithms. We then get the average performance of such 500 groups independently

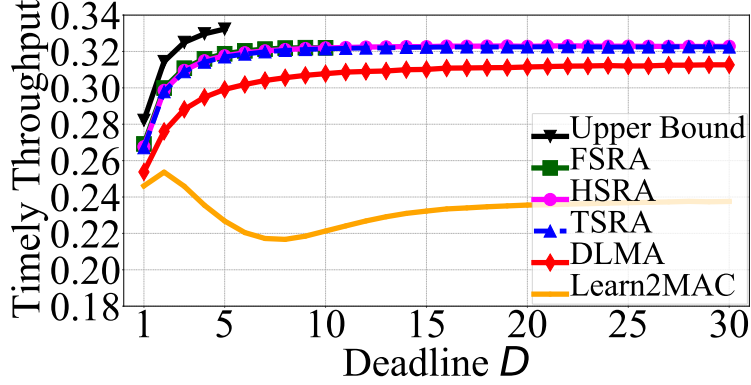


Fig. 5. Comparison of the system timely throughputs of the upper-bound algorithm, FSRA/HSRA/TSRA, and DLMA for the two-device problem.

for the six algorithms. The results are shown in Fig. 5. Note that the state spaces of the upper-bound algorithm and FSRA are of size 2^{2D+2} and 2^{D+2} , respectively, both of which increase exponentially with D . Due to our computational resource limit, we can only evaluate the upper-bound algorithm for $D \leq 5$ and evaluate FSRA for $D \leq 10$. Thus, we can see a truncation for both “Upper Bound” and “FSRA” curves in Fig. 5.

From Fig. 5, we have the following four observations. First, the upper bound proposed in Sec. III indeed provides an effective means for evaluating the timely throughput of different algorithms. This holds by assuming that Device 2 has more revealed information, including Device 1’s parameters and queue information. In addition, we can numerically quantify the performance gap between the upper bound and any other algorithms. For example, the system timely throughput of TSRA (resp. DLMA) is 4.98% (resp. 10.83%) less than that of the upper bound on average for D ranging from 1 to 5. Such a performance gap characterization was missing in many other works applying RL to network communication problems [13], [14], [31]. Second, TSRA has very close performance with HSRA and FSRA. TSRA is only 0.50% worse than FSRA on average for D ranging from 1 to 10, and only 0.15% worse than HSRA on average for D ranging from 1 to 30. This suggests that indeed we can design the R-learning algorithm only depending on whether Device 2 has a most urgent packet (whose lead time is 1). Third, our proposed TSRA for delay-constrained heterogeneous wireless networks achieves better performance than DLMA, which was designed for delay-unconstrained heterogeneous wireless networks. The system timely throughput of TSRA is 5.62% larger than that of DLMA on average

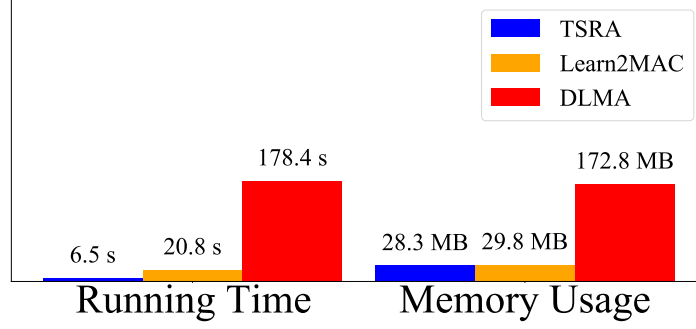


Fig. 6. Comparison of the running times and memory usages of TSRA, Learn2MAC (dictionary size = 100), and DLMA with $D = 10$ for the two-device problem.

for D ranging from 1 to 30. Finally, the Learn2MAC [18] scheme has the worst performance among all schemes. This is because it is designed for homogeneous network, frame-synchronized traffic pattern and perfect channel, all of which do not hold in our system.

Complexity Comparison. In addition to the performance gain in terms of system timely throughput for TSRA over DLMA and Learn2MAC, we further use Fig. 6 to demonstrate that TSRA needs significantly less computational resource than DLMA and Learn2MAC. We run one instance for TSRA, DLMA and Learn2MAC with $p_b = 0.5$, $p'_b = 0.4$, $p_s = 0.7$, $p'_s = 0.6$, $p_t = 0.4$, and $D = 10$. The total number of running slots is 100,000 for all three algorithms. As we can see from Fig. 6, TSRA only needs to run 6.5 seconds, which is 68.75% lower than that of Learn2MAC and 96.36% lower than that of DLMA. And TSRA only needs 28.3 MB of memory, which is a little bit lower than that of Learn2MAC and is 83.62% lower than that of DLMA. The reason is as follows. In terms of time complexity, TSRA only needs to perform two simple computation steps (please refer to (14) and (15)) in each slot. Instead, Learn2MAC needs to update the pattern selection probabilities every D slots and the time complexity depends on the dictionary size (please refer to Step 5 of Algorithm 1 in [18]). The authors in [18] recommend the range of the dictionary size to be 100 to 1000, and we choose the conservative value 100 here. The time complexity could be higher if we choose a larger dictionary size. DLMA needs to go through a fully-connected multilayer neural network with significantly more computation operations in each slot. In terms of space complexity, TSRA only needs to store the scalar ρ and the Q-function table $Q(s, a)$, where s has only 8 possible values and a has only 2 possible

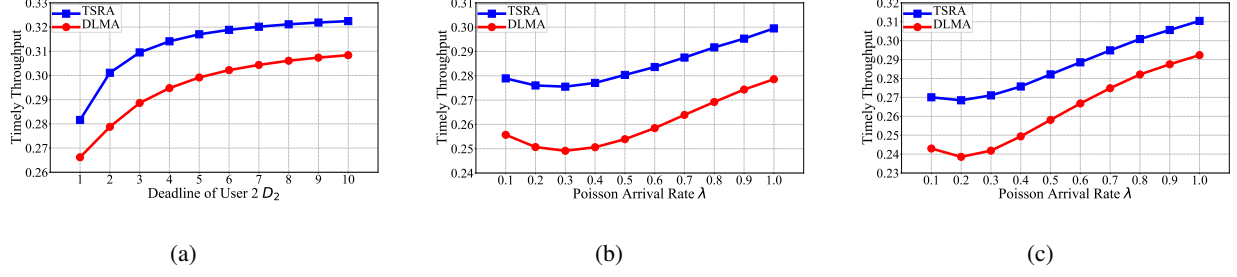


Fig. 7. Robustness results for the two-device problem by comparing the system timely throughputs of TSRA and DLMA. (a) Device 1 and Device 2 have Bernoulli arrivals. We set $D_1 = 5$ and vary D_2 from 1 to 10. (b) Device 1 has Poisson arrivals with $D_1 = 2$ and Device 2 has Bernoulli arrivals with $D_2 = 2$. We vary Poisson arrival rate λ from 0.1 to 1.0. (c) Device 1 has Poisson arrivals with $D_1 = 4$ and Device 2 has Bernoulli arrivals with $D_2 = 2$. We vary Poisson arrival rate λ from 0.1 to 1.0.

values (please refer to Sec. IV). However, DLMA needs to store a memory pool of 500 states, each of which is the collection of transmission events of all past 160 slots, and the parameters of the fully-connected multilayer neural network [13, Table 1].

Robustness. Finally, we demonstrate the robustness of our proposed TSRA algorithm for delay-constrained heterogeneous wireless networks. In this paper, we assume that both devices have Bernoulli arrivals and all their packets have the same hard delay D . We then consider three different settings with larger heterogeneity:

- Case 1 (Different hard delays): Both Device 1 and Device 2 have Bernoulli arrivals, but they have different hard delay D 's (Fig. 7(a));
- Case 2 (Different traffic patterns): Device 1 has Poisson arrivals while Device 2 has Bernoulli arrivals, but they have the same hard delay (Fig. 7(b));
- Case 3 (Different hard delays and different traffic patterns): Device 1 has Poisson arrivals with delay D_1 , while Device 2 has Bernoulli arrivals with a different delay D_2 (Fig. 7(c)).

Note that for each point in Figs. 7(a)-7(c), we get the average among randomly selected 500 groups of system parameters (p_s, p_t, p'_b, p'_s) , each running 100,000 slots. We can observe that TSRA is again better than DLMA for all three cases. On average, the system timely throughput of TSRA is 5.85% more than that of DLMA in Fig. 7(a), 9.30% more than that of DLMA in Fig. 7(b), and 9.02% more than that of DLMA in Fig. 7(c). These results show that our proposed TSRA is robustly better than DLMA for different heterogeneous settings.

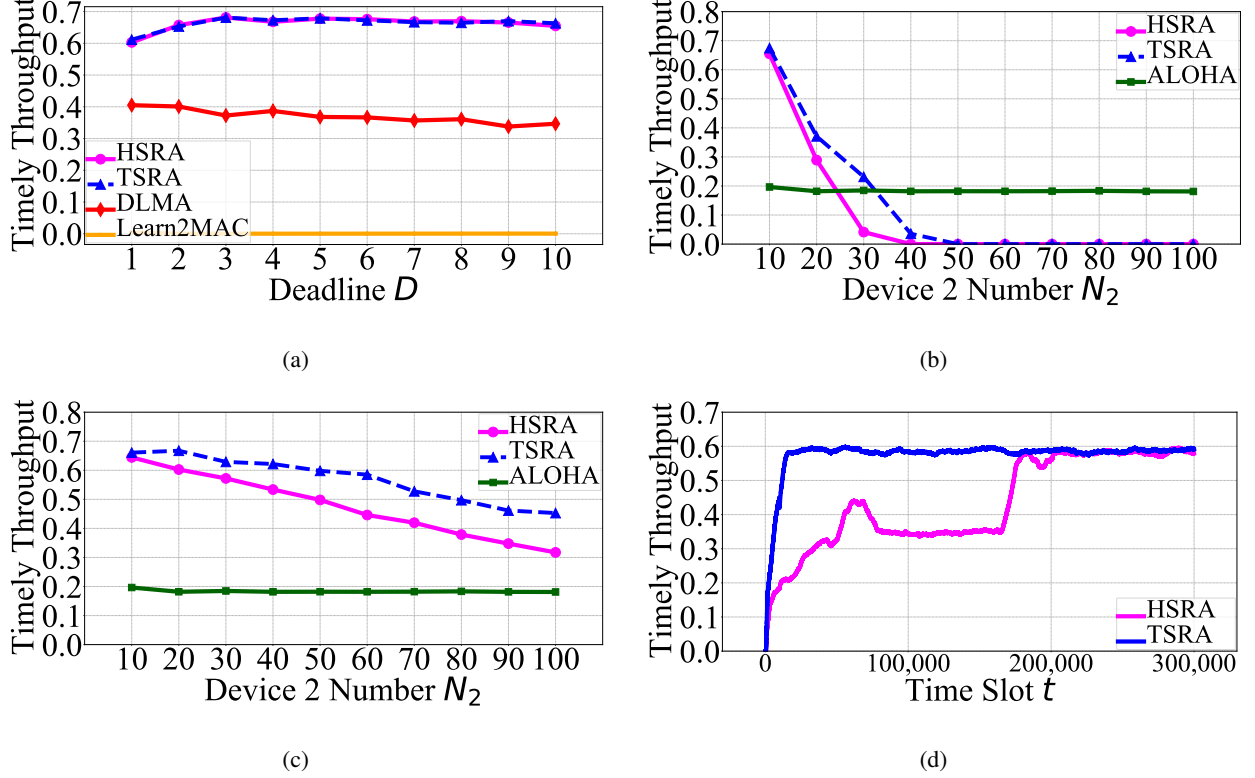


Fig. 8. Comparison of the system timely throughput for the multi-device problem. (a) Compare TSRA, HSRA, and Learn2MAC when $N_1 = 0$, $N_2 = 10$ and D from 1 to 10 with reward function in Table III. (b) Compare TSRA, HSRA, and ALOHA when $N_1 = 0$, $D = 10$ and N_2 varying from 10 to 100 with reward function in (11). (c) Compare TSRA, HSRA, and ALOHA when $N_1 = 0$, $D = 10$ and N_2 varying from 10 to 100 with reward function in Table III. (d) Convergence results of TSRA and HSRA when $N_1 = 0$, $N_2 = 100$ and $D = 10$ with reward function in Table III.

B. Multi-Device Case

We now demonstrate the performance of our proposed schemes for the general multi-device problem. In all simulations in this subsection, we assume that all devices have Bernoulli arrivals.

Timely Throughput Comparison. We first compare TSRA, HSRA, DLMA, and Learn2MAC when $N_1 = 0$ and $N_2 = 10$. Namely, in Fig. 4, there are zero device in the left side and 10 devices in the right side, all of which will use TSRA/HSRA/DLMA/Learn2MAC. We vary the hard delay D from 1 to 10. For each D , we randomly select 100 groups of system parameters and independently run each group for 100,000 slots for all four algorithms. We then get the average performance of such 100 groups independently for the four algorithms. The results are shown in Fig. 8(a). We can see that our proposed TSRA and HSRA achieve the largest system timely throughput than existing baselines, DLMA and Learn2MAC. In addition, TSRA

and HSRA have the same performance. This demonstrates that TSRA/HSRA also works well for the general multi-device problem. Concretely, in this figure, we can see that TSRA increases the system timely throughput by 79.19% as compared with DLMA under the multi-device case. The performance gain is significantly larger than that (only 5.62% in Sec. VI-A) of the two-device case.

Now we increase the number of devices, i.e., N_2 , from 10 to 100 with stepsize of 10 and compare the two schemes, TSRA and HSRA. In Sec. V, we have argued that we should change the reward function from (11) to Table III. To justify this modification, we will independently evaluate TSRA and HSRA for these two different reward functions. As a comparison, we also show the result when all N_2 devices use the simple ALOHA scheme where the transmission/retransmission probability is $1/N_2$ [15]. Fig. 8(b) shows the result with the two-level reward function (i.e., (11)), and Fig. 8(c) shows the result with the modified multi-level reward function (i.e., Table III). We can see that both TSRA and HSRA become worse when the number of devices N_2 increases and even worse than the simple ALOHA scheme when $N_2 \geq 30$ under the two-level reward function (i.e., (11)). However, with the modified multi-level reward function (i.e., Table III), both TSRA and HSRA work better than ALOHA in all cases. Fig. 8(b) and Fig. 8(c) justify why we should modify the reward function for the multi-device problem.

We also obtain a somehow counter-intuitive observation from Fig. 8(c). When N_2 is large, the low-complexity TSRA is even better than the medium-complexity HSRA scheme. As we discussed in Sec. IV-B, HSRA considers the HoL packets while TSRA only considers the most urgent packets. It seems that TSRA losses more system information than HSRA. Thus, TSRA should be worse than HSRA, or at least same as HSRA. It cannot be strictly better than HSRA, as justified by Fig. 5 when $N_1 = 1$ and $N_2 = 1$ and Fig. 8(a) when $N_1 = 0$ and $N_2 = 10$. However, Fig. 8(c) shows that TSRA is strictly better than HSRA when $N_2 \geq 20$. To explain this counter-intuitive observation, in Fig. 8(d), we show the convergence result of TSRA and HSRA when $N_1 = 0$, $N_2 = 100$ and $D = 10$ with reward function in Table III. We can see that HSRA converges much more slowly than TSRA due to its large state space in the multi-device case. Since we only run 100,000 slots, HSRA has not yet converged and thus its system timely throughput is lower than that of the converged TSRA.

Therefore, Fig. 8 demonstrates the superior performance of TSRA with the modified multi-level reward function (i.e., Table III) for the general multi-device problem.

Complexity Comparison. Similar to Fig. 6, we also compare the computation complexity in

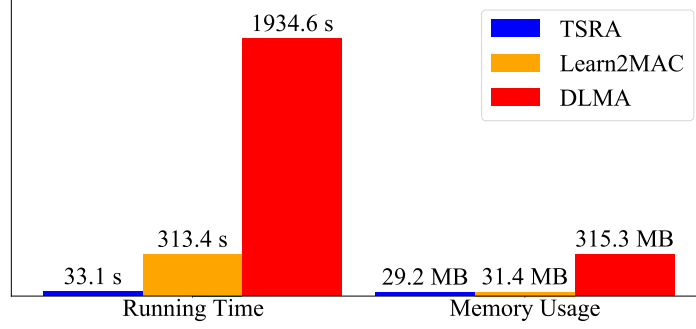


Fig. 9. Comparison of the running times and memory usages of TSRA, Learn2MAC (dictionary size = 100), and DLMA when $N_1 = 0$, $N_2 = 10$ and $D = 10$ for the multi-device problem.

terms of running time and memory usage for TSRA, DLMA and Learn2MAC for the general multi-device problem. We consider $N_1 = 0$, $N_2 = 10$, and $D = 10$. The result is shown in Fig. 9. We can see that, in terms of running time, TSRA needs to run 33.1 seconds, which is 89.44% lower than that of Learn2MAC and 98.29% lower than that of DLMA. In terms of memory usage, TSRA consumes 29.2 MB of memory, which is 7.01% lower than that of Learn2MAC and only 90.74% lower than that of DLMA. This figure shows that TSRA again has much lower computation complexity than existing baselines for the general multi-device problem.

System Power Consumption Comparison. Mobile devices, especially for Internet of Things (IoT) devices, usually have limited battery capabilities and need to work for a long time. Thus, power consumption is a key performance metric for mobile devices. Although in the previous sections, we did not optimize the power consumption, in this part, we will compare the system power consumption of our proposed TSRA scheme and existing baselines, Learn2MAC and DLMA, for general multi-device problem. Same as [18], we define the system power consumption as the average number of devices that transmit a packet per slot, i.e.,

$$P = \lim_{T \rightarrow \infty} \frac{\sum_{t=1}^T \sum_{i \in \mathcal{N}} 1_{\{\text{Device } i \text{ transmits a packet at slot } t\}}}{T}. \quad (23)$$

Note that in (23), we do not model the detailed power consumption in wireless communication, but instead use the average transmission times to reflect the power consumption. Since we do not optimize the power allocation in the physical layer, (23) is a simplified but useful performance metric to evaluate the system power consumption in our problem.

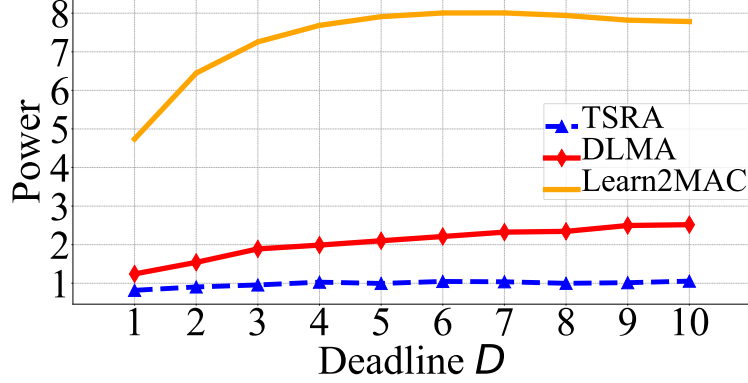


Fig. 10. Comparison of power of TSRA, DLMA, and Learn2MAC when $N_1 = 0$, $N_2 = 10$ and D ranges from 1 to 10 for the multi-device problem.

We consider $N_1 = 0$, $N_2 = 10$ and $D = 10$. The result is shown in Fig. 10. The system power consumption of TSRA is $0.99 \approx 1$, which is 52.29% lower than that of DLMA and 86.60% lower than that of Learn2MAC. This is the best result for random access: if there is one and only one device transmits a packet in each slot, the system can fully utilize the channel without causing collision. Thus, TSRA can best collaborate with each other to fully utilize the channel in a distributed manner. On the contrary, the system power consumption of Learn2MAC is 7.36, implying that on average 7.36 devices transmit a packet per slot. Thus, collision happens in almost all slots. This also explains why the system timely throughput of Learn2MAC is almost 0 in Fig. 8(a). The system power consumption of DLMA is significantly lower than Learn2MAC, but still larger than twice of our proposed TSRA scheme.

Effect of Different Uncontrollable Congestion Levels. As we discussed in Sec. V, we first considered the important case of $N_1 = 0$. Thus, all previous simulations in this subsection is based on $N_1 = 0$. But it is also very important to see the performance of TSRA when $N_1 > 0$. Recall that N_1 is the number of uncontrollable ALOHA devices (see Fig. 4) in our considered heterogeneous wireless network. In this part, we demonstrate the effect of different uncontrollable congestion levels by considering $N_1 = 1, 2$ and 3.

We assume that all N_1 uncontrollable devices has a new packet arrival every slot (i.e., the arrival probability is 1 under the Bernoulli traffic model). In addition, the transmission probabilities of them are set as $\frac{1}{4N_1}$ and the channel success probabilities are set as 0.5. We independently simulate both $N_2 = 0$ and $N_2 > 0$. Note that $N_2 = 0$ means that there are only

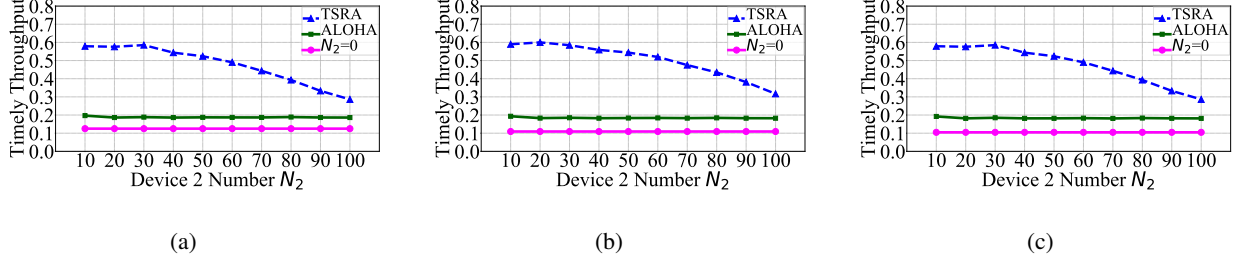


Fig. 11. Comparison of system timely throughput of TSRA and ALOHA when $N_2 \in \{0\} \cup [10, 100]$ and $D = 10$ with different N_1 values (i.e., different uncontrollable congestion levels) for the multi-device problem. Note that $N_2 = 0$ means that there is zero device in the right side of Fig. 4, which is the magenta curve in the figure. (a) $N_1 = 1$. (b) $N_1 = 2$. (c) $N_1 = 3$.

N_1 uncontrollable devices in the system. It can provide a benchmark to gauge the performance change of adding extra TSRA/ALOHA devices (i.e., $N_2 > 0$). For $N_2 > 0$, we assume that such N_2 controllable devices deploy TSRA or ALOHA (with transmission probability $\frac{1}{N_2}$). For each N_1 and N_2 , we randomly select 100 groups of system parameters and independently run each group for 100,000 slots for TSRA and ALOHA. We then get the average performance of such 100 groups independently for TSRA and ALOHA. The result is shown in Fig. 11. We remark that we cannot run DLMA in our computer platform as DLMA has much higher time and space complexity (see Fig. 9). In addition, the performance of Learn2MAC is very bad with almost zero system timely throughput (see Fig. 8(a)). Thus, we do not have DLMA and Learn2MAC results in Fig. 11.

We can see that in all cases, TSRA achieves much higher system timely throughput (on average 161.16% among all cases) than the simple ALOHA scheme. In addition, comparing with the case $N_2 = 0$ (the magenta curve in Fig. 11), adding extra N_2 ALOHA devices can increase the system timely throughput by 63.85% on average among all cases, while adding extra N_2 TSRA devices can significantly increase the system timely throughput by 327.90% on average among all cases. Therefore, our proposed TSRA allows controllable devices to smartly collaborate with uncontrollable devices and can opportunistically utilize the channel to further improve the system timely throughput.

VII. CONCLUSION

In this paper, we for the first time investigate the random access problem for delay-constrained heterogeneous wireless networks. We propose an R-learning-based low-complexity algorithm,

called TSRA. We show that TSRA achieves higher timely throughput, lower computation complexity, and lower power consumption simultaneously than the existing baseline DLMA [13], which was designed for delayed-unconstrained heterogeneous wireless networks.

Three key messages have been delivered by this work. First, although RL has been widely used in many network decision problems, few works characterize their performance gap due to RL's black-box nature. In this work, for the simple two-device case, we instead propose an MDP-based formulation to derive a model-based upper bound such that it can numerically quantify the performance gap of any RL-based scheme. We believe that this methodology can benefit other network problems utilizing RL. Second, since network problems are concerned with throughput or timely throughput, which is by nature an average reward, it is revealed by this work that average-reward-based R-learning is better than the currently widely-used discounted-reward-based Q-learning. Finally, for delay-constrained communications, we show that the most urgent packets have the biggest impact on the system performance, which can be utilized to simplify the system design significantly.

For future research of this ongoing work, it is interesting and important to consider the device fairness, whilst maximizing the system timely throughput.

REFERENCES

- [1] D. Wu, L. Deng, Z. Liu, Y. Zhang, and Y. S. Han, "Reinforcement learning random access for delay-constrained heterogeneous wireless networks: A two-user case," in *Proc. IEEE GLOBECOM Workshop on Towards Native-AI Wireless Networks*, 2021, pp. 1–7.
- [2] 3GPP TS 22.104, Service requirements for cyber-physical control applications in vertical domains, 2020.
- [3] K.-C. Chen, S.-C. Lin, J.-H. Hsiao, C.-H. Liu, A. F. Molisch, and G. P. Fettweis, "Wireless networked multirobot systems in smart factories," *Proceedings of the IEEE*, vol. 99, no. PP, pp. 1–27, 2020.
- [4] G. P. Fettweis, "The tactile Internet: Applications and challenges," *IEEE Vehicular Technology Magazine*, vol. 9, no. 1, pp. 64–70, 2014.
- [5] K. Kim and P. R. Kumar, "Cyber-physical systems: A perspective at the centennial," *Proceedings of the IEEE*, vol. 100, no. Special Centennial Issue, pp. 1287–1308, 2012.
- [6] L. Deng, C. Wang, M. Chen, and S. Zhao, "Timely wireless flows with general traffic patterns: Capacity region and scheduling algorithms," *IEEE/ACM Transactions on Networking*, vol. 25, no. 6, pp. 3473–3486, 2017.
- [7] L. Deng, C. Tan, F. Zhang, and W. S. Wong, "Joint design of control policy and network scheduling policy for wireless networked control systems: Theory and application," *Information Sciences*, vol. 575, pp. 563–586, 2021.
- [8] R.-A. Koutsiamanis, G. Z. Papadopoulos, X. Fafoutis, J. M. Del Fiore, P. Thubert, and N. Montavont, "From best effort to deterministic packet delivery for wireless industrial IoT networks," *IEEE Transactions on Industrial Informatics*, vol. 14, no. 10, pp. 4468–4480, 2018.
- [9] L. Leonardi, F. Battaglia, and L. L. Bello, "RT-LoRa: A medium access strategy to support real-time flows over LoRa-based networks for industrial IoT applications," *IEEE Internet of Things Journal*, vol. 6, no. 6, pp. 10 812–10 823, 2019.

- [10] M. S. Elbamby, C. Perfecto, M. Bennis, and K. Doppler, "Toward low-latency and ultra-reliable virtual reality," *IEEE Network*, vol. 32, no. 2, pp. 78–84, 2018.
- [11] DARPA spectrum collaboration challenge (SC2). [Online]. Available: <https://archive.darpa.mil/sc2/>.
- [12] P. Tilghman, "Will rule the airwaves: A DARPA grand challenge seeks autonomous radios to manage the wireless spectrum," *IEEE Spectrum*, vol. 56, no. 6, pp. 28–33, 2019.
- [13] Y. Yu, T. Wang, and S. C. Liew, "Deep-reinforcement learning multiple access for heterogeneous wireless networks," *IEEE Journal on Selected Areas in Communications*, vol. 37, no. 6, pp. 1277–1290, 2019.
- [14] Y. Yu, S. C. Liew, and T. Wang, "Non-uniform time-step deep Q-network for carrier-sense multiple access in heterogeneous wireless networks," *IEEE Transactions on Mobile Computing*, vol. 20, no. 9, pp. 2848–2861, 2021.
- [15] L. Deng, J. Deng, P. Chen, and Y. S. Han, "On the asymptotic performance of delay-constrained slotted ALOHA," in *Proc. IEEE ICCCN*, 2018, pp. 1–8.
- [16] Y. Zhang, Y. Lo, F. Shu, and J. Li, "Achieving maximum reliability in deadline-constrained random access with multiple-packet reception," *IEEE Transactions on Vehicular Technology*, vol. 68, no. 6, pp. 5997–6008, 2019.
- [17] C. Campolo, A. Molinaro, A. Vinel, and Y. Zhang, "Modeling prioritized broadcasting in multichannel vehicular networks," *IEEE Transactions on Vehicular Technology*, vol. 61, no. 2, pp. 687–701, 2011.
- [18] A. Destounis, D. Tsilimantos, M. Debbah, and G. S. Paschos, "Learn2MAC: Online learning multiple access for URLLC applications," in *Proc. IEEE INFOCOM Workshops*, 2019, pp. 1–6.
- [19] A. Schwartz, "A reinforcement learning method for maximizing undiscounted rewards," in *Proc. ACM ICML*, 1993, pp. 298–305.
- [20] S. P. Singh, "Reinforcement learning algorithms for average-payoff Markovian decision processes," in *Proc. AAAI*, 1994, pp. 700–705.
- [21] R. S. Sutton and A. G. Barto, *Reinforcement Learning: An Introduction*. MIT Press, 2018.
- [22] A. Dua, "Random access with multi-packet reception," *IEEE Transactions on Wireless Communications*, vol. 7, no. 6, pp. 2280–2288, 2008.
- [23] J. Sun, Z. Jiang, B. Krishnamachari, S. Zhou, and Z. Niu, "Closed-form Whittle's index-enabled random access for timely status update," *IEEE Transactions on Communications*, vol. 68, no. 3, pp. 1538–1551, 2019.
- [24] H. H. Yang, C. Xu, X. Wang, D. Feng, and T. Q. Quek, "Understanding age of information in large-scale wireless networks," *IEEE Transactions on Wireless Communications*, vol. 20, no. 5, pp. 3196–3210, 2021.
- [25] I. Hou, V. Borkar, and P. Kumar, "A theory of QoS for wireless," in *Proc. IEEE INFOCOM*, 2009.
- [26] I. Hou and P. Kumar, "Scheduling heterogeneous real-time traffic over fading wireless channels," in *Proc. IEEE INFOCOM*, 2010.
- [27] —, "Utility maximization for delay constrained QoS in wireless," in *Proc. IEEE INFOCOM*, 2010.
- [28] M. L. Puterman, *Markov Decision Processes: Discrete Stochastic Dynamic Programming*. John Wiley & Sons, Inc., 1994.
- [29] A. Hordijk and L. Kallenberg, "Linear programming and Markov decision chains," *Management Science*, vol. 25, no. 4, pp. 352–362, 1979.
- [30] F. Zhang, A. Gong, L. Deng, and Y. Zhang, "Scheduling algorithms for wireless downlink with deadline and retransmission constraints," in *Proc. IEEE ICCT*, 2020, pp. 736–740.
- [31] N. C. Luong, D. T. Hoang, S. Gong, D. Niyato, P. Wang, Y.-C. Liang, and D. I. Kim, "Applications of deep reinforcement learning in communications and networking: A survey," *IEEE Communications Surveys & Tutorials*, vol. 21, no. 4, pp. 3133–3174, 2019.

APPENDIX

A. Proof of Theorem 1

For $D = 1$, as we explained in Sec. III, all slots are decoupled such that we only need to focus on one particular slot. Thus, we can shrink our design space to a single parameter, i.e., the transmission probability of Device 2, which is denoted by p'_t . To optimize p'_t , we first define the following random variables:

- Random variable $A_i, i = 1, 2$:

$$A_i = \begin{cases} 1, & \text{Device } i \text{ has a non-expired packet to transmit;} \\ 0, & \text{otherwise.} \end{cases} \quad (24)$$

- Random variable $X_i, i = 1, 2$:

$$X_i = \begin{cases} 1, & \text{Device } i \text{ transmits a packet;} \\ 0, & \text{otherwise.} \end{cases} \quad (25)$$

- Random variable $Y_i, i = 1, 2$:

$$Y_i = \begin{cases} 1, & \text{Device } i \text{ transmits a packet successfully;} \\ 0, & \text{otherwise.} \end{cases} \quad (26)$$

Then, given parameters $p_b, p'_b, p_s, p'_s, p_t, p'_t$, we can derive the distributions for the above random variables. The system timely throughput is,

$$R = \mathbb{E}[Y_1 + Y_2] = \mathbb{E}[Y_1] + \mathbb{E}[Y_2] = P(Y_1 = 1) + P(Y_2 = 1). \quad (27)$$

Next we compute $P(Y_1 = 1)$ as follows,

$$\begin{aligned} P(Y_1 = 1) &= \sum_{x_1 \in \{0,1\}} \sum_{x_2 \in \{0,1\}} P(Y_1 = 1 | X_1 = x_1, X_2 = x_2) P(X_1 = x_1, X_2 = x_2) \\ &= P(Y_1 = 1 | X_1 = 1, X_2 = 0) P(X_1 = 1, X_2 = 0) \end{aligned} \quad (28)$$

$$= p_s \cdot P(X_1 = 1, X_2 = 0) \quad (29)$$

$$= p_s \cdot P(X_1 = 1) \cdot P(X_2 = 0), \quad (30)$$

where (28) holds because Device 1 can deliver a packet successfully only if Device 1 transmits a packet and Device 2 does not transmits a packet in the considered slot, and (29) holds because the transmission events of both devices are independent.

Now let us again use the law of total probability to compute $P(X_1 = 1)$ and $P(X_2 = 0)$ in (30),

$$\begin{aligned}
 P(X_1 = 1) &= \sum_{a_1 \in \{0,1\}} P(X_1 = 1|A_1 = a_1)P(A_1 = a_1) \\
 &= P(X_1 = 1|A_1 = 1)P(A_1 = 1) \\
 &= p_t p_b,
 \end{aligned} \tag{31}$$

$$\begin{aligned}
 P(X_2 = 0) &= \sum_{a_2 \in \{0,1\}} P(X_2 = 0|A_2 = a_2)P(A_2 = a_2) \\
 &= P(X_2 = 0|A_2 = 0)P(A_2 = 0) + P(X_2 = 0|A_2 = 1)P(A_2 = 1) \\
 &= 1 \cdot (1 - p'_b) + (1 - p'_t) \cdot p'_b \\
 &= 1 - p'_b p'_t.
 \end{aligned} \tag{32}$$

Inserting (31) and (32) into (30), we obtain that

$$P(Y_1 = 1) = p_s p_t p_b (1 - p'_t p'_b). \tag{33}$$

Similarly, we can obtain

$$P(Y_2 = 1) = p'_s p'_t p'_b (1 - p_t p_b). \tag{34}$$

Inserting (33) and (34) into (27), we obtain the system timely throughput as,

$$\begin{aligned}
 R &= p_s p_t p_b (1 - p'_t p'_b) + p'_s p'_t p'_b (1 - p_t p_b) \\
 &= [p'_s - (p_s + p'_s) p_t p_b] p'_t p'_b + p_s p_t p_b.
 \end{aligned}$$

Thus, if

$$p_t p_b < \frac{p'_s}{p_s + p'_s}, \tag{35}$$

the optimal p'_t to maximize the system timely throughput R is

$$p'_t = 1, \tag{36}$$

i.e., Device 2 will always transmit its packet if it has one packet. Otherwise, if (35) does not hold, the optimal p'_t to maximize the system timely throughput R is

$$p'_t = 0, \tag{37}$$

i.e., Device 2 will never transmit its packet. This completes the proof.

B. Why is FSQA worse than FSRA and how to improve FSQA?

As we showed in Fig. 2, the Q-learning-based FSQA algorithm is worse than the R-learning-based FSRA. In this part, we consider a specific example for the two-device problem to delve into the details of FSQA and FSRA. We set system parameter settings as $p_b = 0.5$, $p'_b = 0.4$, $p_s = 0.7$, $p'_s = 0.6$, $p_t = 0.4$, $D = 2$. The achieved system timely throughput of FSQA and FSRA is show in Fig. 12. Obviously, FSRA outperforms FSQA. Now we take a further step to examine the random access policies of FSQA and FSRA, which are shown in Table IV. As we can see, indeed, after convergence, FSQA and FSRA take different policies, which thus results in different system timely throughput.

It is not clear which policy is better. We then use the upper-bound policy as a benchmark, i.e., (9), to justify that the policy of FSRA is better. Note that in the upper-bound algorithm, we use a model-based MDP formulation where Device 2 is aware of Device 1's queue information and parameters. Thus, different from FSQA and FSRA whose system state is $s = (l_2, o)$ as shown in (10), the system state of the upper-bound algorithm also includes Device 1's queue information, i.e., $s = (l_1, l_2, o)$, as shown in (4). The policy of the upper-bound algorithm is shown in Table V. Each state of FSQA and FSRA, i.e., $s = (l_2, o)$, corresponds to four states of upper-bound policy, i.e., $s = (l_1, l_2, o)$ where $l_1 \in \{(0, 0), (0, 1), (1, 0), (1, 1)\}$. For such four states of the upper-bound policy sharing the same l_2 and o , we take a vote to obtain the majority action, which is the last column in Table V. The majority action roughly represents the optimal action if the Device 2's queue information is l_2 and the channel observation is o . We compare the majority action of the upper-bound policy in Table V and the action of FSRA and FSQA in Table IV. We can see that FSRA has exactly the same action with the upper-bound policy for all states, while FSQA has different actions for four states $(l_2, o) = ((1, 0), \text{SUCCESSFUL})$, $((1, 1), \text{BUSY})$, $((1, 1), \text{SUCCESSFUL})$, and $((1, 1), \text{FAILED})$. With the help of the model-based upper-bound policy as a benchmark, we can see that indeed the policy of R-learning-based FSRA is better than the policy of Q-learning-based FSQA.

Furthermore, we also use this example to show how to improve the performance of Q-learning-based FSQA algorithm. Comparing the Q-function update of Q-learning in (12) and the Q-function update of R-learning in (14), we can see that the major difference is the parameter ρ . Comparing (13) and (17), which respectively represents the physical meaning of Q-function for Q-learning and R-learning, we can also observe that for average-reward MDP, we should use a

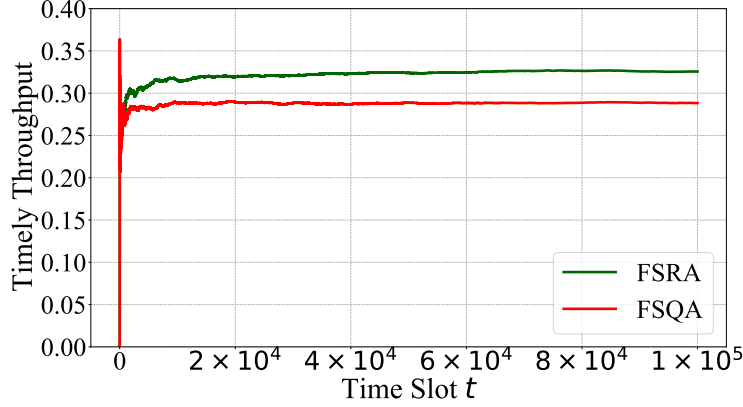


Fig. 12. Compare the timely throughput of FSRA and FSQA where $p_b = 0.5$, $p'_b = 0.4$, $p_s = 0.7$, $p'_s = 0.6$, $p_t = 0.4$, $D = 2$.

relative value to response the reward. Namely, the reward should be deducted by a constant ρ . To improve the Q-learning-based FSQA algorithm, we thus re-define its reward function in (11) as

$$r(s_t, a_t) \triangleq 1_{\{o_t \in \{\text{BUSY}, \text{SUCCESSFUL}\}\}} - c, \forall s_t \in \mathcal{S}', a_t \in \mathcal{A}, \quad (38)$$

where $c \in [0, 1]$ is a constant. We then compare the performance of FSRA and the improved FSQA algorithms with different c 's, as shown in Fig. 13. As we can see, when constant $c = 0.3$, the improved FSQA achieves almost the same system timely throughput with FSRA, which is much better the original FSQA algorithm (with $c = 0$). In fact, parameter ρ in (15) of FSRA converges to 0.379 in this example. Thus, the optimal constant $c = 0.3$ in the improved FSQA is close to the converged ρ of FSRA. Although we can improve FSQA by re-defining its reward function according to (38), there is generally no guidance on how to choose the best constant c , which is different for different problem instances. Instead, in R-learning-based FSRA, the parameter ρ is algorithmically adjusted according to (15) until its convergence. This further demonstrates the benefit of R-learning over Q-learning for our studied problem.

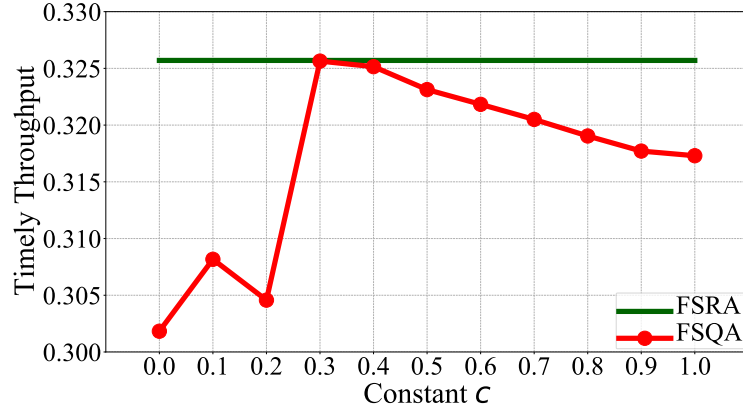


Fig. 13. Compare the timely throughput of FSRA and the improved FSQA where $p_b = 0.5$, $p'_b = 0.4$, $p_s = 0.7$, $p'_s = 0.6$, $p_t = 0.4$, $D = 2$.

TABLE IV

THE POLICIES OF FSRA AND FSQA AFTER CONVERGENCE WHEN $p_b = 0.5$, $p'_b = 0.4$, $p_s = 0.7$, $p'_s = 0.6$, $p_t = 0.4$ AND $D = 2$. NOTE THAT CHANNEL OBSERVATION $o = \text{B}$ MEANS THAT $o = \text{BUSY}$, $o = \text{S}$ MEANS THAT $o = \text{SUCCESSFUL}$, $o = \text{I}$ MEANS THAT $o = \text{IDLE}$, AND $o = \text{F}$ MEANS THAT $o = \text{FAILED}$.

State		FSRA	FSQA
$s = (l_2, o)$		action	
l_2	o	a	
(0,0)	B	WAIT	WAIT
(0,0)	S	WAIT	WAIT
(0,0)	I	WAIT	WAIT
(0,0)	F	WAIT	WAIT
(0,1)	B	TRANSMIT	TRANSMIT
(0,1)	S	TRANSMIT	TRANSMIT
(0,1)	I	TRANSMIT	TRANSMIT
(0,1)	F	TRANSMIT	TRANSMIT
(1,0)	B	TRANSMIT	TRANSMIT
(1,0)	S	TRANSMIT	WAIT
(1,0)	I	TRANSMIT	TRANSMIT
(1,0)	F	TRANSMIT	TRANSMIT
(1,1)	B	TRANSMIT	WAIT
(1,1)	S	TRANSMIT	WAIT
(1,1)	I	TRANSMIT	TRANSMIT
(1,1)	F	TRANSMIT	WAIT

TABLE V

THE UPPER-BOUND POLICY (9) WHEN $p_b = 0.5$, $p'_b = 0.4$, $p_s = 0.7$, $p'_s = 0.6$, $p_t = 0.4$ AND $D = 2$. NOTE THAT CHANNEL OBSERVATION $o = B$ MEANS THAT $o = \text{BUSY}$, $o = S$ MEANS THAT $o = \text{SUCCESSFUL}$, $o = I$ MEANS THAT $o = \text{IDLE}$, AND $o = F$ MEANS THAT $o = \text{FAILED}$.

State			$\pi(s a)$		Majority
$s = (l_1, l_2, o)$			a		
l_1	l_2	o	WAIT	TRANSMIT	
(0,0)	(0,0)	B	1	0	WAIT
(0,1)			1	0	
(1,0)			1	0	
(1,1)			1	0	
(0,0)	(0,0)	S	1	0	WAIT
(0,1)			1	0	
(1,0)			1	0	
(1,1)			1	0	
(0,0)	(0,0)	I	1	0	WAIT
(0,1)			1	0	
(1,0)			1	0	
(1,1)			1	0	
(0,0)	(0,0)	F	1	0	WAIT
(0,1)			1	0	
(1,0)			1	0	
(1,1)			1	0	
(0,0)	(0,1)	B	0	1	TRANSMIT
(0,1)			0	1	
(1,0)			1	0	
(1,1)			0	1	
(0,0)	(0,1)	S	0	1	TRANSMIT
(0,1)			0	1	
(1,0)			1	0	
(1,1)			0	1	
(0,0)	(0,1)	I	0	1	TRANSMIT
(0,1)			0	1	
(1,0)			1	0	
(1,1)			0	1	
(0,0)	(0,1)	F	0	1	TRANSMIT
(0,1)			0	1	
(1,0)			1	0	
(1,1)			0	1	
(0,0)	(1,0)	B	0	1	TRANSMIT
(0,1)			0	1	
(1,0)			0.47916	0.52084	
(1,1)			0.49551	0.50449	
(0,0)	(1,0)	S	0	1	TRANSMIT
(0,1)			0	1	
(1,0)			0	1	
(1,1)			0	1	
(0,0)	(1,0)	I	0	1	TRANSMIT
(0,1)			0	1	
(1,0)			0.35845	0.64155	
(1,1)			0.43222	0.56778	
(0,0)	(1,0)	F	0	1	TRANSMIT
(0,1)			0	1	
(1,0)			0	1	
(1,1)			0	1	
(0,0)	(1,1)	B	0	1	TRANSMIT
(0,1)			0	1	
(1,0)			0.49072	0.50928	
(1,1)			0.49713	0.50287	
(0,0)	(1,1)	S	0	1	TRANSMIT
(0,1)			0	1	
(1,0)			0	1	
(1,1)			0	1	
(0,0)	(1,1)	I	0	1	TRANSMIT
(0,1)			0	1	
(1,0)			0.41202	0.58798	
(1,1)			0.44799	0.55201	
(0,0)	(1,1)	F	0	1	TRANSMIT
(0,1)			0	1	
(1,0)			0	1	
(1,1)			0	1	